TRANSACTIONS OF THE INSTITUTE OF MEASUREMENT & CONTROL

Article

Transactions of the Institute of Measurement and Control
2018, Vol. 40(7) 2259–2269

DOI: 10.1177/0142331217700241
journals.sagepub.com/home/tim
SAGE

Event-triggered and self-triggered wide-area damping control designs under uncertainties

Jiajun Duan[1], Hao Xu[2] and Wenxin Liu[1]

Abstract

Traditional damping controllers of wide-area power systems (WAPSs) are not able to solve the inter-area oscillation problem effectively owing to lack of global vision. It weakens the power transfer capability and even the stability of WAPSs. The installation of a large number of phase measurement units brings about the system-wide synchronized measurements. Considering that conventional periodic control solutions have placed an excessive burden on the cyber infrastructure, in this paper, two advanced aperiodic control schemes are designed based on the real-time global synchronized measurements. Two control schemes, that is, zero-order-hold event-triggered control and self-triggered control, are developed for wide-area damping control with the minimum communication between the control center and the actuators. The control center only updates control signals for the actuators when certain conditions are triggered, and there is no communication occurrence for the rest of time. Thus, they have mild requirements on communication and computation. The algorithms are tested through simulations of WAPS models with different levels of details. The simulation results demonstrate the effectiveness and benefits of the control design.

Keywords

Wide-area control, wide-area power system, event-triggered control, self-triggered control, inter-area oscillation, power system stabilizer

Introduction

With the growth of power grid, regional power systems are interconnected through weak tie-lines, that is, long distance transmission lines, to form the so-called wide-area power systems (WAPSs). The Western Electricity Coordinating Council (WECC) system in the US and the South & Central China Grid are typical examples of WAPSs (Chakrabortty et al., 2012; Ma et al., 2011; Taylor et al., 2005). The benefits of the WAPSs include the establishment of mutual backup, enhanced redundancy and increased capability and efficiency of generation allocation (Chakrabortty et al., 2011; Taylor et al., 2005). However, WAPSs are difficult to manage owing to the wide coverage size and the complex interactions among subsystems.

In past years, there has been a huge investment in wide-area measurement systems (WAMSs). A large number of phasor measurement units (PMUs) have been deployed in the North American grid as well as many other countries all over the world (Chakrabortty et al., 2011; Dorler et al., 2014). PMUs bring about synchronized dynamic data, which make the advanced wide-area monitoring and control possible. There have been many successful applications of open-loop wide-area monitoring systems. But the closed-loop control of WAPSs is challenging owing to the complexity of WAPS and uncertainties with both cyber and physical systems. To fully unlock the potentials brought by the WAMSs, advanced wide-area control methods should be comprehensively studied. The corresponding research requires the integration of multi-disciplinary expertise, especially in power and control.

One challenging problem of WAPSs is the existence of the inter-area oscillations, which lowers power transfer capability and even system stability. Insufficient damping efforts could result in severe consequences with huge losses, such as the notorious power outage accident of WECC system on 10 August 1996 (Chakrabortty et al., 2012). Traditional solutions to this problem include installing conventional power system stabilizers (CPSSs) to generate auxiliary damping signals to the excitation system of a synchronous generator. CPSSs are designed using the theory of phase compensation in the frequency domain and are introduced as lead-lag compensators (Kishor et al., 2012). Owing to the lack of global vision and difficulty with parameter tuning, CPSSs cannot provide satisfactory damping performance for WAPSs (Zhang et al., 2012). With the deployment of WAMSs, more and more studies have been conducted to design sophisticated controllers for WAPSs using wide-area measurements.

In the work of Ma et al. (2011), a collocated control algorithm-based global power system stabilizer design is introduced. Damping is realized by excluding the eigenvalues

[1]Department of Electrical and Computer Engineering, Lehigh University, Bethlehem, PA, USA
[2]Department of Electrical and Biomedical Engineering, University of Nevada, Reno, NV, USA

Corresponding author:
Wenxin Liu, Department of Electrical and Computer Engineering, Lehigh University, Bethlehem, PA, USA.
Email: wel814@lehigh.edu

of system dynamics that are corresponding to low frequency oscillations. In the work of Wu et al. (2008), the remote generator rotor speed is used as an extra input to the CPSSs and the control gain is obtained with linear matrix inequalities method. The authors also consider time delay of communication and data processing. In order to adapt to changes in WAPSs, model prediction adaptive control is introduced to enhance the stability of WAPSs by Wang and Cheung (2008). In the work of Hui et al. (2002), authors propose a multi-agent system based wide-area damping scheme. Robust control and fuzzy logics are used to design the supervisory level damping controller. A similar two-level control scheme is presented by Okou et al. (2005), which enhances local damping control through a wide-area nonlinear control with adaptation module. Instead of designing new algorithms, a model decomposition based algorithm is proposed by Zhang et al. (2012). It focuses on tuning CPSSs to damp the concerned inter-area mode without significantly compromising of other oscillation modes. The performance of above-mentioned algorithms is generally validated through simulation, such as with the 2-area 4-machine power system model (Kundur, 1994).

However, above wide-area control algorithms require continuous calculation and deployment of the control signals. Implementation of this type of solutions requires high bandwidth communications. With increased integration of distributed/renewable generators, the communication systems need to deliver more data to counteract the uncertainties over a wide range of operating conditions. To avoid communication jam (Dib et al., 2009) or high investment on communication system upgrade (Mazo and Tabuada, 2011), it is desirable to design advanced control solutions that have relaxed communication requirements while still maintaining the desired control performance. In this way, more bandwidth can be saved and used for other control functions.

Since event-triggered and self-triggered controls only update control signals when it is necessary, they are promising control solutions for wide-area damping control (Sahoo et al., 2013). The concepts of two control techniques are quite similar and the differences can be found in (Sahoo et al., 2016). These two control techniques have been introduced to study various control systems (Zhang et al., 2016) including power systems. In the work of Xiao et al. (2011), self-triggered control is applied to excitation system of synchronous generator to reduce calculation requirements. Event-triggered control is applied to reduce the communication requirement of the traditional load frequency controller (Wen et al., 2016). In the work of Tahir and Mazumder (2015), the self-triggered control is also used in microgrids for generation dispatch among multiple distributed generators. However, there is currently no application of event-triggered or self-triggered control method applied in damping control of WAPSs.

In this paper, two communication-inexpensive control algorithms are designed for wide-area damping control based on the continuously available PMU data from the WAMSs. The two control algorithms are designed based on zero-order hold (ZOH) event-triggered and self-triggered control techniques, respectively. By properly designing the triggering conditions, the amount of communication between the control center and the actuators can be significantly reduced. The proposed control algorithms are first tested with a linearized 11-bus-4-machine power system model in presence of uncertain model parameters and small load fluctuations. In order to estimate their real-world performance, the algorithms are also tested with a non-linear detailed model under large disturbances. Simulation results illustrate that the proposed algorithms are not only effective for damping wide-area oscillations, but also economical in term of communication and computation requirements.

The contributions and merits of this paper are summarized as follows. First, a novel ZOH event-triggered controller design and a ZOH self-triggered controller are proposed for wide-area damping control of WAPSs, respectively. Although event-triggered and self-triggered controls have been studied recently, it is the first time that they are applied into WAPSs' damping control. Second, the event-triggering and self-trigging conditions are developed considering both time-varying modeling uncertainties and system disturbances. Third, simulation studies with WAPSs models of different levels of details demonstrate that the proposed algorithms can provide effective inter-area oscillation damping while significantly decreasing computation and communication requirements.

Background

WAPSs

The interconnected WAPSs have several advantages. First, the reliability of the overall system can be improved. If some contingencies occur in one subsystem, it has a better chance to survive under supports of other subsystem(s) (Taylor et al., 2005). Second, the energy efficiency of the overall system can be enhanced. Since a subsystem could receive low-cost power supply from other subsystems, the overall operation cost of the system can be reduced (Leon et al., 2012). Third, the flexibility of the power grid can be increased. Because subsystems can work autonomously similar to micro-grid power systems, the inter-connected tie lines can be intentionally disconnected under extreme conditions to avoid the spreading of wide-area blackouts (Chakrabortty et al., 2011).

However, WAPSs are difficult to control owing to the wide coverage area and complex interactions among subsystems. Traditional power systems are controlled based on local information and tend to make myopic decisions. The installation of PMUs brings the real-time global vision to control centers for wide-area monitoring and controlling. Owing to the difficulty with closed-loop control of the complex WAPSs, the development of wide-area control schemes has been lagging the hardware investment. So far, the major application of PMUs is still on the open-loop wide-area monitoring and diagnosis. It is necessary to study the challenging closed-loop control problems of the WAPSs and to unlock the potentials of the installed PMUs.

Event-triggered and self-triggered controls

Currently, the periodic control schemes are widely used in the traditional power systems (Hui et al., 2002; Kishor et al., 2012; Wen et al., 2016; Xiao et al., 2011). Such periodic control schemes require expensive computation cost and large

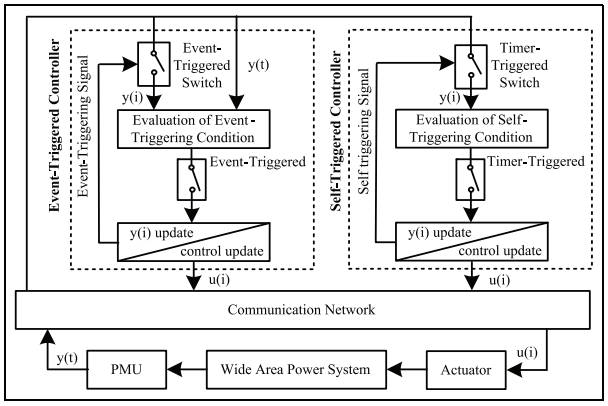

Figure 1. Illustration of ZOH event-triggered or self-triggered controls systems.

communication bandwidth to support the data exchanges among PMUs, controllers and actuators. To meet the ever-increasing expectations and requirements of the smart grid, more and more control functions will be added. If periodic control schemes continue to be used, WAPSs might eventually be overloaded owing to its limited computation and network resources (Dib et al., 2009).

In order to reduce the communication requirements, the aperiodic control techniques, that is, the event-triggered and the self-triggered controls, can be introduced. The flow chart of the two control techniques is illustrated in Figure 1. The basic idea behind them is to update control signals only when certain conditions are triggered. The certain conditions are designed to strictly maintain the system stability (Garcia and Antsaklis 2011). During the time period without control updating, previously applied control signal in the actuator is kept being used. In this way, only necessary communications are incurred between the control center and the actuators.

As shown in Figure 1, both controllers use measurements of PMUs to generate control signals for the actuators implementation. For event-triggered control, a previous system measurement $y(i)$ is recorded and compared with the real-time measurement $y(t)$ continuously. If the deviation between the two signals is larger than a predefined threshold, an event will be triggered. Under such conditions, both system output $y(i)$ and control signal $u(i)$ will be updated. For self-triggered control, the triggering signal is a timer, whose setting is calculated based on the previous system measurement $y(i)$ and the stability requirement. The operations after the self-triggering condition being triggered are similar to that of event-triggered control.

The objectives of both control techniques are to maintain the stability of system while minimizing computation and communication requirements. The major difference is with confidence or assumptions of system's operating conditions. Self-triggered control assumes system's operating condition does not change abruptly and tries to maximize updating intervals. In comparison, event-triggered control does not make assumptions on operating conditions but takes action whenever necessary. Statically, self-triggered control has lower requirements on communication but might not adapt to severe changes of system operating conditions in a timely manner. The event-triggered control can provide a timely response, but requires continuous monitoring of system's operating conditions. For the specific wide-area damping control application that assumes the availability of WAMSs, the requirement of online monitoring of event-triggered control can be easily accommodated. Based on above analysis, one can see that the event-triggered and the self-triggered control techniques have certain advantages and disadvantages of themselves. In this paper, both control techniques have been introduced for wide-area damping controller designs.

WAPSs with ZOH event-triggered and self-triggered control

Modeling of WAPSs

Effective modeling of a WAPS is challenging owing to its complexity. To simplify wide-area control design, a subsystem (regional power system) can be modeled as an aggregated generator based on the coherent theory (Kundur, 1994). Multiple such subsystems are then connected together to form a WAPS. Extensive PMUs are deployed for grid-wide synchronized measurement, which is used for wide-area monitoring and control.

The WAPS model used in the control design is modified based on the small-signal model proposed by Chakrabortty et al. (2011, 2012). This WAPS model integrates the dynamics of synchronous generators (SGs), static loads, and transmission lines. By introducing Kron reduction to eliminate all buses except for generator terminal buses, the original differential-algebraic-equation-based model can be transformed into a complete dynamic model (Chakrabortty and Khargonekar, 2013) as shown in equation (1).

$$\begin{cases} \dot{x}(t) = f(x(t), u(t)) \\ y(t) = g(x(t)) \end{cases} \tag{1}$$

In equation (1), $x(t) = \left[\delta^T \omega^T E^T\right]^T$ is a column vector of the states of the WAPS with δ being a column vector of the rotor angle deviations, ω being a column vector of the angular speed deviations, and E being a column vector of the internal generated voltages, respectively. $u(t) = \left[{P_m}^T {E_f}^T\right]^T$ is a column vector of the control signals to the WAPS with P_m being a column vector of the mechanical power outputs of the turbines and E_f being a column vector of the field voltage outputs of the exciters. $y(t) = \left[\theta^T 2\pi f^T V^T\right]^T$ are the PMU measurements on generator terminal buses where V is the column vector of bus voltage, θ and f are the column vectors of bus voltage phase angle and frequency, respectively.

To further simplify the above WAPS model for control design, similar linearization (Kishor et al., 2012) can be performed around an equilibrium operating point $x_0 = [\delta_0 \omega_0 E_0]^T$ that satisfies $f(x_0, u_0) = 0$. By introducing the time-invariant matrices $A = \frac{\partial f}{\partial x}|_{(x_0, u_0)}$ and $B = \frac{\partial f}{\partial u}|_{(x_0, u_0)}$, the linearized system dynamics can be represented as

$$\Delta\dot{x}(t) = A\Delta x(t) + B\Delta u(t) \tag{2}$$

where the deviations are defined as $\Delta x(t) = x(t) - x_0$ and $\Delta u(t) = u(t) - u_0$. The matrices of $A \subset \mathbb{R}^{n\times n}$ and $B \subset \mathbb{R}^{n\times m}$ can be calculated based on the parameters and initial (equilibrium) states of the WAPS.

Since an SG's internal states ($\Delta\delta$ and ΔE) are not directly measurable, PMUs are usually deployed on generator terminal buses to measure V, θ, and f. According to the work of Chakrabortty and Khargonekar (2013), the following relationship exists between the PMUs measurements ($\Delta\theta$, Δf and ΔV) and SG's states ($\Delta\delta$, $\Delta\omega$, andΔE).

$$y(t) = \begin{bmatrix} \Delta V(t) \\ \Delta\theta(t) \\ \Delta f(t) \end{bmatrix} = \begin{bmatrix} F_1 & F_2 & 0 \\ F_3 & F_4 & 0 \\ 0 & 0 & \omega_s G \end{bmatrix} \begin{bmatrix} \Delta E(t) \\ \Delta\delta(t) \\ \Delta\omega(t) \end{bmatrix} = C\Delta x(t) \tag{3}$$

where $C = \begin{bmatrix} F_1 & F_2 & 0 \\ F_3 & F_4 & 0 \\ 0 & 0 & \omega_s G \end{bmatrix}$ is a non-singular square matrix with F_i and G being constant blocks calculated based on the equilibrium operating point x_0 and parameters of SGs. The detailed expressions of C is omitted in this paper owing to the limitation in space; interested readers can refer to the papers of Chakrabortty et al. (2012, 2013). Because the square matrix C is constant and invertible, the states $\Delta x(t)$ can be estimated by using output multiplying a constant gain as $\Delta x(t) = C^{-1}\Delta y(t)$. Thus, the state space representation in equation (2) can be rewritten using outputs $\Delta y(t)$ as

$$\Delta\dot{y}(t) = A_y\Delta y(t) + B_y\Delta u(t) \tag{4}$$

where $A_y = CAC^{-1} \subset \mathbb{R}^{n\times n}$ and $B_y = CB \subset \mathbb{R}^{n\times m}$. Because the inaccuracies introduced during modeling, linearization and measurement approximation are unavoidable, they should be addressed properly. Thus, the linearized dynamic model for wide-area control design can be represented as

$$\Delta\dot{y}(t) = \left[A_y + \Delta A(t)\right]\Delta y(t) + \left[B_y + \Delta B(t)\right]\Delta u(t) + D(t) \tag{5}$$

where $D(t)$ denotes the time-varying disturbances,$\Delta A(t)$ and $\Delta B(t)$ represent the time-varying uncertainties in the system. It should be mentioned that the formulation of equation (5) has been widely used to present parameter uncertainties in many physical systems (Hu et al., 2012). Besides, uncertainties and disturbances are assumed to be bounded; that is, $\Delta A(t) \le a_u$, $\Delta B(t) \le b_u$ and $D(t) \le D_M$ (Garcia and Antsaklis 2011). The introduction of uncertainties and disturbances makes the linearized model applicable to a wider range of operating conditions. However, owing to uncertainties, the control design becomes more difficult and challenging. To overcome this deficiency, novel ZOH event-triggered and self-triggered control designs are developed and introduced in next subsections.

Event-triggered and self-triggered control designs

In this section, novel ZOH event-triggered and self-triggered wide-area control algorithms that can maintain WAPS stability under uncertainties and disturbances are presented. First, the event-triggering condition under ideal case (i.e. system without uncertainties and disturbances) is derived. Then, a more realistic case (i.e. system with uncertainties and disturbances) are considered to design event-triggered control and self-triggered control separately.

The proposed ZOH control law can be formulated as

$$\Delta u(t) = \begin{cases} K\Delta y(i) & \textit{event or time condition is not triggered} \\ K\Delta\, y(t) & \textit{event or time condition is triggered} \end{cases}, \; 0 < iT_s \le t \tag{6}$$

where T_s is the sampling time, and K is the feedback control gain so that the closed-loop system matrix $\left(A_y - B_yK\right)$ are negative definite. If the event triggering condition or time triggering condition is activated, control signals will be adjusted using the most recent measurements. Otherwise, previously updated control is used until the condition is triggered again. For linear systems with known system dynamics – that is, those that can be formulated as equation (4)–K can be obtained by solving the following Lyapunov equation (7) as proposed by Sahoo et al. (2013).

$$\left(A_y + B_yK\right)^TP + P\left(A_y + B_yK\right) = -Q \tag{7}$$

where Q and P are positive definite matrices.

Theorem 1: (Event-triggering Condition under Ideal Case): Under the ideal situation – that is, the system dynamics are precisely known – the event-triggering condition can be designed as

$$\|e(t)\| < \gamma_{ideal}\|\Delta y(t)\| \tag{8}$$

where $e(t) = \Delta y(i) - \Delta y(t)$ is the error between the previously recorded output deviation $\Delta y(i)$ and the current output deviation $\Delta y(t)$, $\gamma_{ideal} = \sigma\frac{q}{2\left[K^TB_y^TP\right]}$ is the threshold coefficient with $q = \lambda_{min}(Q)$ being the minimum eigenvalues of Q. σ is designed parameter which satisfy $0 < \sigma < 1$. Also, Q and P can be obtained by solving Lyapunov equation given in (7)

Proof: Refer to Appendix.

However, in practice, system uncertainties and disturbances always exist. They could affect the system performance and complicate the even-triggering condition design significantly. Therefore, the bounds of system uncertainties and disturbances (a_u, b_u and D_M) are used to design the event-triggering and self-triggering conditions. For linear systems subjecting to disturbances and uncertainties – that is, those can be represented with equation (5)– the event-triggering condition defined as equation (8) has to be updated to maintain stability.

Design of event-triggering condition under uncertainties and disturbances

Theorem 2: (Event-triggering Condition under Realistic Case): Inspired by the stability analysis in the work of Lewis et al. (1999), the ZOH event-triggered control in equation (6) for WAPS formulated as equation (5) can guarantee the system state deviations being uniformly ultimately bounded (UUB) under the event-triggering condition of equation (9) as

$$\|e(t)\| < \gamma_T\|\Delta y(t)\| \tag{9}$$

where $\gamma_T = \sigma \frac{(q-\Phi)}{2\left[K^T B_y^T P + K^T b_u P\right]}$ is the proposed threshold coefficient with Φ and q defined according to $\Phi = 2\|P\|(a_u + b_u\|K\|)$ and $q = \lambda_{min}(Q)$, respectively. To maintain the stability of control system, the following condition in terms of P, Q, K, a_u, *and* b_u should be satisfied

$$\Phi < q \tag{10}$$

The boundedness of $\Delta y(t)$ is represented as equation (11)

$$\Delta y(t) \leq \sqrt{\frac{b_e}{(1-\sigma)(q-\Phi)}} \tag{11}$$

where $b_e > 0$ is defined as $b_e = \frac{2}{\sigma(q-\Phi)} D_M P$.

Proof: Refer to Appendix.

Design of self-triggering condition under uncertainties and disturbances

Based on equation (5), the relationship between $\Delta y(t)$ and $\Delta y(i)$ can be represented as equation (12).

$$\begin{aligned} e(t) &= \Delta y(i) - \Delta y(t) \\ &= -\int_i^{i+\Delta t} \left\{\left[A_y + \Delta A(s)\right]\Delta y(s) + \left[B_y + \Delta B(s)\right]\Delta u(s) + D(s)\right\} ds \\ &\cong \left\{\left[A_y + \Delta A(i)\right]\Delta y(i) + \left[B_y + \Delta B(i)\right]\Delta u(i) + D(i)\right\}\Delta t \end{aligned} \tag{12}$$

According to equation (12), one can have $\|e(t)\| = \left\|\left\{\left[A_y + \Delta A(i)\right]\Delta y(i) + \left[B_y + \Delta B(i)\right]\Delta u(i) + D(i)\right\}\right\|\|\Delta t\|$ and $\|\Delta y(t)\| = \|\Delta y(i)\| - \left\|\left\{\left[A_y + \Delta A(i)\right]\Delta y(i) + \left[B_y + \Delta B(i)\right]\Delta u(i) + D(i)\right\}\right\|\|\Delta t\|$. Based on the event-triggering condition of equation (9), the self-triggering condition can be derived as

$$\Delta t < \frac{\gamma_T \|\Delta y(i)\|}{(1-\gamma_T)\left\|\left[A_y + a_u\right]\Delta y(i) + \left[B_y + b_u\right]\Delta u(i) + D_M\right\|} \tag{13}$$

Owing to the existence of model uncertainties and disturbances, asymptotic stability cannot be realized. The control accuracy – that is, the bound of $\Delta y(t)$– is decided by the extent of model accuracy and magnitude of disturbance. During control implementation, the designed parameters P and Q can be selected based on the estimation of $\Delta A(t)$ and $\Delta B(t)$ firstly. Then, control gain K is calculated according to (7) together with selected P and Q, practical $\Delta A(t)$ and $\Delta B(t)$ can be used to check the validity of equation (10). If needed, P, Q and K can be redesigned.

Because the difficulty with bound estimation of $\Delta A(t)$ and $\Delta B(t)$, it is not easy to decide the best triggering condition accurately; that is, the maximum interval between instants of time when the two sequential conditions get triggered. In order to maintain the stability over a wide range of operating conditions, more stringent triggering condition (smaller triggering interval) can be selected. The triggering interval increases with the increase of certainty and accuracy of model. The design of event-triggering and self-triggering conditions are trade-off between stability confidence and communication requirement. The existence of nonzero lower bound of the event-triggering interval can be proven similar as the work of Sahoo et al. (2016).

Simulation studies

It is common sense that the actual model of a large-scale power system is very complex and highly nonlinear. Owing to the complexity, it is difficult to obtain an accurate model of such a system. An accurate model is desirable for simulation study but might be inconvenient for controller design. To design a simple yet effective algorithm, model simplification is necessary. However, the algorithm based on the simplified model must be tested with a more accurate and detailed model to estimate its real-world performance.

In order to evaluate the performance of the linear-based control designs, they are tested with both linearized model and detailed nonlinear WAPS models such as the Kundur model (Kundur, 1994). As introduced earlier, this model has been extensively used to test new algorithms and to analyze practical power systems. The implementation diagram of the proposed control algorithm is illustrated in Figure 2. Wide-area measurements (i.e. voltage phase angle θ, rotor speed f and generator terminal voltage V) are measured using PMUs. The sampling interval T_s is 0.1s. The central controller, which implements the event-triggered or self-triggered algorithm separately, decides when to update the global measurements and the control signals.

Simulation results with linearized model

The control algorithm is designed based on the linearized model. However, the designed controller uses real-world measurements during implementation. Owing to the limited accuracy of the linearized model, the real-world measurements deviate from the controller's expectation predicted from the linearized model. To counteract the mismatch between the predicted and measured data (the inaccuracy of the linearized model), up to 5% parameter deviations ($\Delta A(t)$ and $\Delta B(t)$) of the linearized system parameter matrixes are simulated. In addition, up to 5% disturbance ($D(t)$) is simulated to investigate the effectiveness of the designed algorithm under small and continuous load fluctuations. For initialization, small random noises are also added to system states to further disrupt the system.

The damping performance of the event-triggered control design under such conditions is illustrated in Figure 3. Among the three plots, Figure 3(a) shows the response of bus voltage phase angle deviation ($\Delta\theta$), Figure 3(b) shows the response of frequency deviation (Δf), and Figure 3(c) shows the response of terminal bus voltage deviation (ΔV), all in per-unit values. Owing to the time-varying system uncertainties and load changes, there are always small oscillations in the bus voltage phase angel deviations, frequency deviations, and terminal bus voltage deviations. Considering the units used in figures are per unit values, the oscillations are reasonably small and acceptable.

The control signal responses of event-triggered control are illustrated in Figure 4. Since the control responses of the four

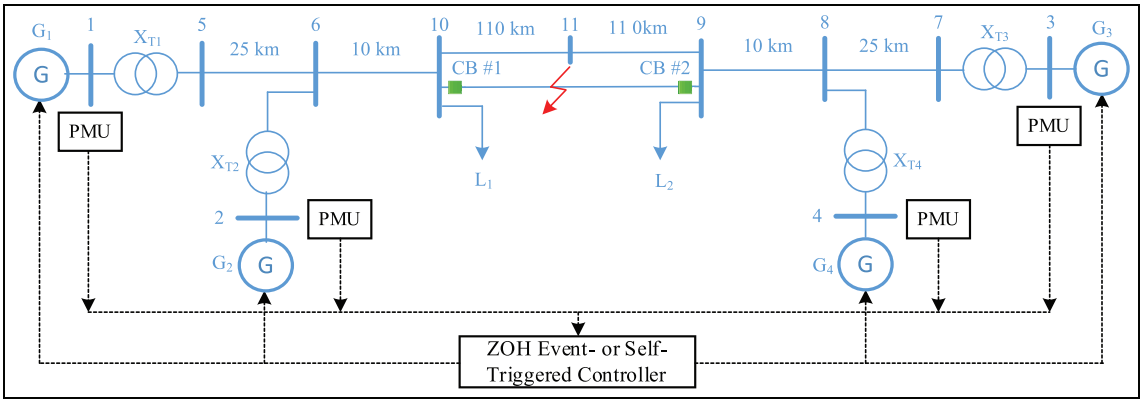

Figure 2. Implementation of the proposed controller with the 4-generator model.

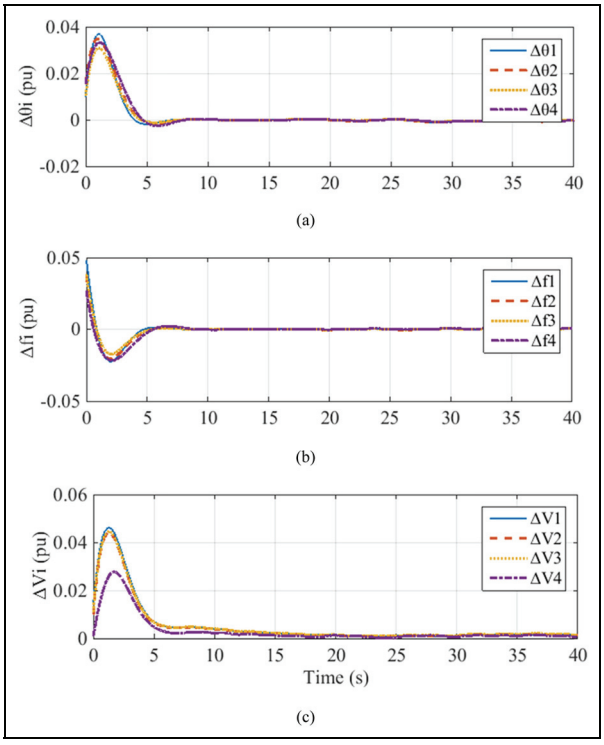

Figure 3. Simulation results of the proposed event-triggered controller with linearized model: (a) phase angle deviation ($\Delta\theta$); (b) frequency deviations (Δf); (c) terminal bus voltage deviations (ΔV).

SGs are similar, only the control signals (ΔE_{f1} and ΔP_{m1}) of SG #1 are plotted. It can be seen that the control signals also oscillate around zero owing to model parameter inaccuracy and continuous load fluctuations. Because of the small size of disturbance, the control actions are not triggered continuously. Previous control signals are held fixed until control is triggered again. It is the reason that step changes of the control signals can be observed.

Similarly, the damping performance of the self-triggered control design under same conditions is presented in Figure 5. Among the five plots, Figure 5(a) shows the response of voltage phase angle deviation ($\Delta\theta$), Figure 5(b) shows the

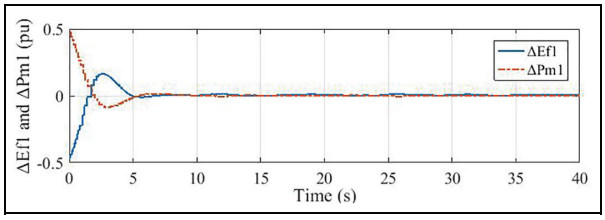

Figure 4. Wide-area damping control signals of generator #1 with event-triggered controller (adjustments of field voltage and mechanical power input).

response of frequency deviation (Δf), and Figure 5(c) shows the response of terminal bus voltage deviation (ΔV), all in per-unit values. The control signal responses of SG #1 are illustrated in Figure 6.

The computational effort comparison among continuously-updated control scheme, the event-triggered control scheme and self-triggered control scheme is visualized in Figure 7, which shows the accumulated numbers of control updates at different instants of time. Since the time interval T_s is set up as 0.1 seconds for periodic control, the total numbers of control updates of the continuously-updated control increase linearly from 0 to 400 after 40 seconds. In comparison, the response of event-triggered control increases slowly after the control system is stabilized within a small region From Figure 7, it is clearly to see the benefit of event-triggered or self-triggered control designs in term of communications savings. It should be noted that because the self-triggered controller calculates the next triggering time based on a predefined system model, it can usually save more communications than an event-triggered controller. But the damping performance of self-triggered controller may degrade if the system is suffering big time-varying disturbances.

Simulation results with nonlinear detailed model

To evaluate the performance of the proposed event-triggered and self-triggered controllers in a real application, the algorithms are tested with the detailed model of WAPS. The specific objectives include testing the algorithm under large

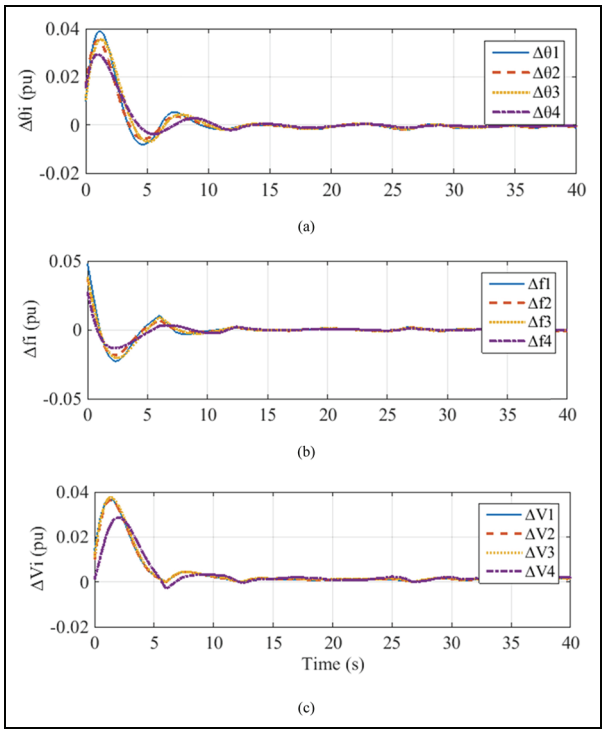

Figure 5. Simulation results of the proposed self-triggered controller with linearized model: (a) phase angle deviation ($\Delta\theta$); (b) frequency deviations (Δf); (c) terminal bus voltage deviations (ΔV).

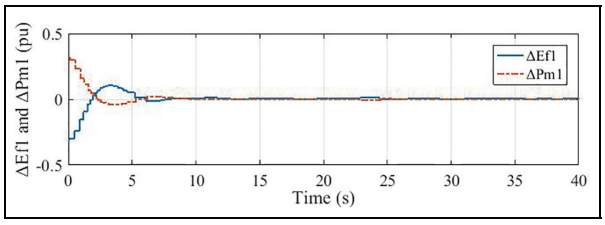

Figure 6. Wide-area damping control signals of generator #1 with self-triggered controller (adjustments of field voltage and mechanical power input).

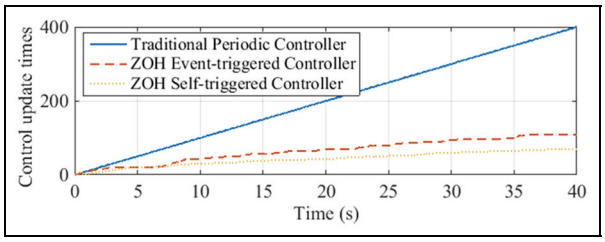

Figure 7. The accumulated numbers of control updates of continuously-updated control, event-triggered control and self-triggered control.

disturbance and comparing its performance against well-tuned CPSSs. The Simulink model that comes with the SimPowerSystem^{TM} toolbox for inter-area oscillations is used for simulation studies. The implantation diagram of the proposed control algorithms with the detailed WAPS model is illustrated in Figure 8.

The event-triggered or self-triggered centralized controller takes the wide-area measurements from PMUs, and then generates the corresponding control signals ΔE_{fi} and ΔP_{mi} aperiodicaly based on certain triggering conditions. It is known that these two control signals, ΔE_{fi} and ΔP_{mi} (physical quantities), have to be realized by the physical components (exciters and turbines). Because the electrical controller (exciter) has a fast response speed and the inertial delay can be ignored, only a gain $1/K_{Ei}$ is added before the exciter. However, the inertial of mechanical controller (turbine) introduces significant delay to ΔP_{mi}. Thus, a simple lead compensator is used based on the turbine dynamics to counteract the delay. Because the generator internal states ($\Delta\delta$andΔE) are not directly measurable, the generator terminal bus measurements ($\Delta\theta$ and ΔV) are used to estimate the states. Since model inaccuracies and disturbances have been considered during controller design, the impact of using terminal voltage on control performance can be minimized.

For the simulation of the proposed event-triggered or self-triggered controller, other inter-area damping controllers (e.g. CPSSs) are not used, but the frequency controller (governor) and voltage controller (automatic voltage regulator - AVR) are still applied. To better evaluate the performance of the proposed control algorithms, the same power system model and the same disturbances are simulated again under the control of CPSSs. During the simulation, four well-tuned CPSSs are deployed to four generators respectively.

In the simulation study, a series of operating condition changes are simulated. Initially, the simulation is running stably. At three seconds, a step load increase (from 967 MW to 1167 MW) at bus #10 is performed. At five seconds, the load at bus #10 is changed back to its original value (967 MW). At 10 seconds, a 3-phase short-circuit fault is simulated on the transmission line connecting buses #9 and #10. After 6-cycles, the fault is cleared by opening the two circuit breakers located at the ends of the transmission line, as shown in Figure 2.

The simulation results of frequency responses (f) under aforementioned circumstances are shown in Figure 9, among which Figure 9(a) presents the control performance using the event-triggered controller, Figure 9(b) is the damping result using self-triggered controller and Figure 9(c) is the control performance under CPSSs, all in per units.

Similarly, the terminal voltages responses (V) are shown in Figure 10, among which Figure 10(a) presents the control performance using the event-triggered controller, Figure 10(b) is the damping result using self-triggered controller and Figure 10(c) is the control performance under CPSSs, all in per units.

From Figure 9 and Figure 10, one can see that measurements from the detailed model do not have much impact on the performance of the designed control algorithm based on the linearized model. This is because the system parameter uncertainties and disturbances have been addressed during modeling.

Even if the CPSSs shown in Figure 9(c) and Figure 10(c) can also stabilize system under load change and fault

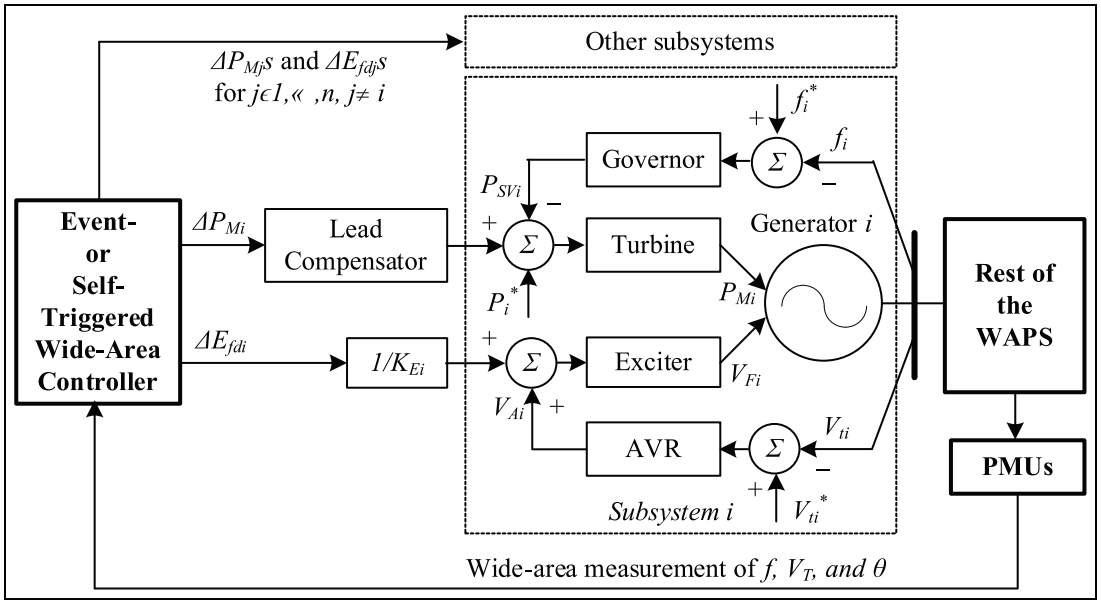

Figure 8. Illustration of the implantation of ZOH event-triggered and self-triggered control for WAPSs.

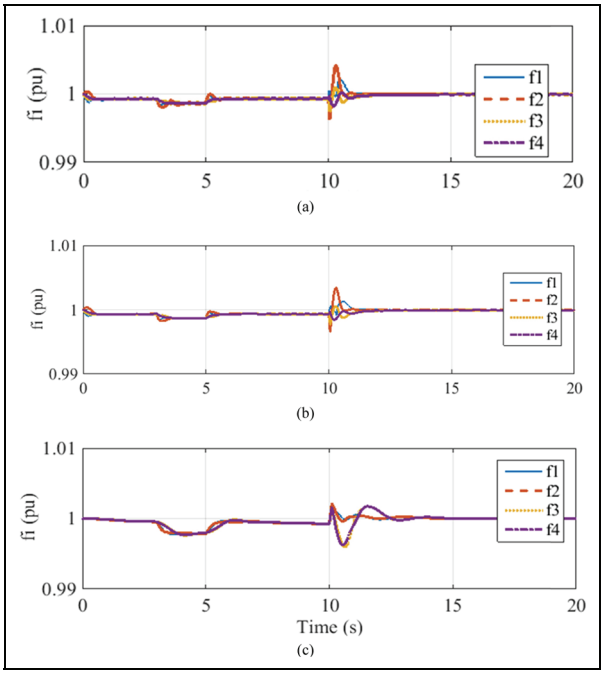

Figure 9. Frequency responses (*f*) under system disturbances, (a) the event-triggered controller; (b) the self-triggered controller; (c) CPSS.

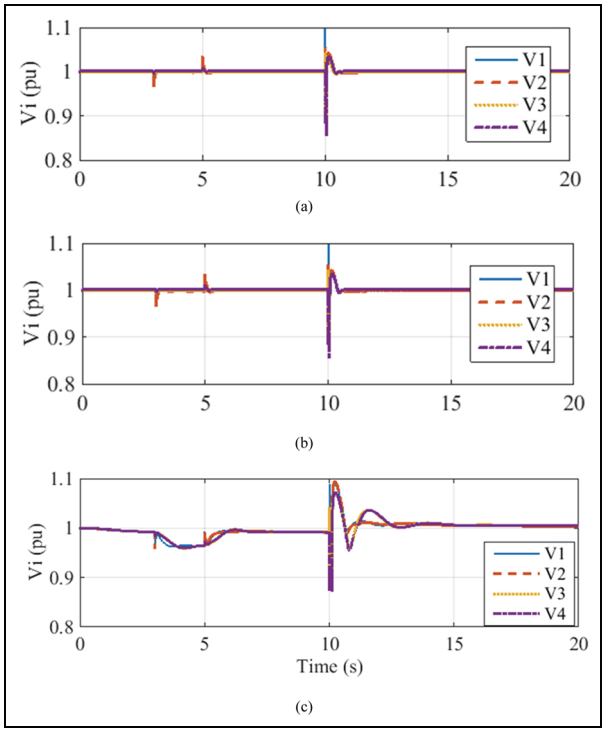

Figure 10. Terminal voltages responses (*V*) under system disturbances, (a) the event-triggered controller; (b) the self-triggered controller; (c) CPSS.

situation, it takes five seconds to damp out oscillations caused by the line fault. While the proposed event-triggered or self-triggered controller only takes less than three seconds to realize the system stabilization. It is because that the proposed wide-area damping controller considers the overall system model and uses the synchronized wide-area data from PMUs (Okou et al., 2005; Chakrabortty and Khargonekar, 2013).

The mechanical control outputs (ΔP_{m1}) of the event-triggered and self-triggered controller for generator #1 are shown in the Figure 11. Among two plots, Figure 11(a) shows the mechanical input power adjustments (ΔP_{m1}) using to

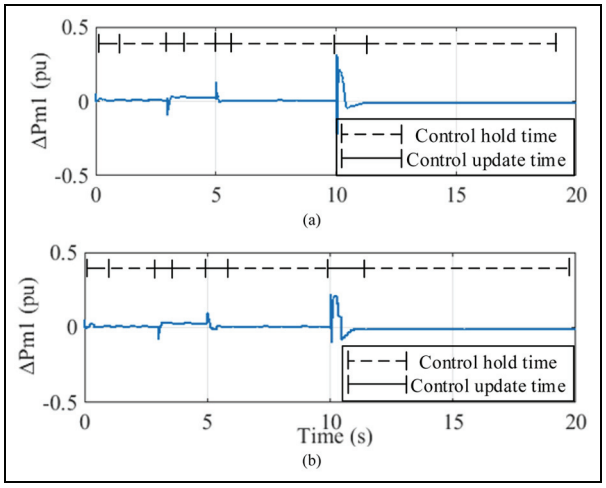

Figure 11. Mechanical control output adjustments ΔP_{m1} of generator #1, (a) event-triggered control; (b) self-triggered control.

event-triggered control while Figure 11(b) is under self-triggered controller. From Figure 11, one can see that the both controllers do not require continuous communications and control updates. In addition, the durations of control activation are decided by the severities of disturbances. The duration is smaller under smaller disturbances (load changes) and larger under larger disturbances (3-phase short-circuit fault). For protection purpose, ramp rates and bounds are applied to the overall control inputs. The control constraints actually introduce more system uncertainties. Obviously, the control constraints do not degrade control performance significantly.

Above simulation results demonstrate the effectiveness of the proposed wide-area damping control algorithm. Even though the algorithm is designed based on the linearized model, the obtained performance is not compromised. Practical control applications prefer such simple yet effective algorithms.

Conclusion

To take advantage of large-scale PMU deployment and avoid overloading control infrastructure, this paper presents an event-triggered and self-triggered control scheme for wide-area oscillation damping. Instead of updating measurements and controls periodically as the traditional control scheme, the proposed control schemes only require such updates when a certain condition is triggered. Thus, they can significantly reduce the requirements on communication. Even though the algorithms are designed based on a linearized model, both parameter uncertainties and system disturbances have been considered. The proposed algorithm is tested with both linearized model and detailed nonlinear model of a 4-generator WAPS. Simulation results show that the two control algorithms can realize effective damping control performance with reduced communication requirements for control implementation.

More and more PMUs are being installed to the modern power grid. However, the benefit of the large investment and capable units have not been fully unlocked. This paper uses the WAMS data to realize closed-loop control and to reduce communication requirements by introducing the event-triggering and self-triggering conditions. Some implementation issues are also considered. However, the simulation studies are conducted with aggregated single-generator subsystem models instead of multiple-generator subsystem models. There are still many open problems of WAPSs on modeling, control design and evaluation to investigate.

Declaration of conflicting interest

The authors declare that there is no conflict of interest.

Funding

This research received no specific grant from any funding agency in the public, commercial or not-for-profit sectors.

References

Chakrabortty A (2012) Wide-area damping control of power systems using dynamic clustering and TCSC-based redesign. *IEEE Transactions on Smart Grid* 3(3): 1503–1514.

Chakrabortty A and Khargonekar PP (2013) Introduction to wide-area monitoring and control. In: *American Control Conference*, Washington, DC, USA, 17–19 June 2013, pp. 6758–6770.

Chakrabortty A, Chow JH and Salazar A (2011) A measurement-based framework for dynamic equivalencing of large power systems using wide area phasor measurements. *IEEE Transactions on Smart Grid* 2(1): 68–81.

Dib W, Ortega R, Barabanov A and Lamnabhi-Lagarrigue F (2009) A globally convergent controller for transient stability of multi-machine power systems using structure preserving models. *IEEE Transactions on Automatic Control* 54(9): 2179–2185.

Garcia E and Antsaklis PJ (2011) Model-based event-triggered control with time-varying network delays. In: *IEEE Conference on Decision and Control and European Control Conference*, Orlando, FL, USA, 12–15 December 2011, pp. 1650–1655.

Hu S, Yin X, Zhang Y and Tian EG (2012) Event-triggered guaranteed cost control for uncertain discrete-time networked control systems with time-varying transmission delays. *IET Control Theory and Applications* 6(8): 2793–2804.

Hui N, Heydt GT and Mili L (2002) Power system stability agents using robust wide area control. *IEEE Transactions on Power Systems* 17(4): 1123–1131.

Kishor N, Haarla L, Turunen J and Larsson M (2012) Wide-area control of power systems through delayed network communication. *IEEE Transactions on Control System Technology* 20(2): 495–503.

Kundur P (1994) *Power Systems Stability and Control*. New York: McGraw-Hill.

Leon AE, Mauricio JM, Gomez-Exposito A and Solsona JO (2012) Hierarchical wide-area control of power systems including wind farms and FACTS for short-term frequency regulation. *IEEE Transactions on Power Systems* 27(4): 2084–2092.

Lewis FL, Jagannathan S and Yesildirek A (1999) *Neural Network Control of Robot Manipulators and Nonlinear Systems*. London: Taylor & Francis.

Ma J, Wang T and Wu J (2011) Design of global power systems stabilizer to damp inter-area oscillations based on wide-area collocated

control technique. In: *2011 IEEE Power and Energy Society General Meeting*, San Diego, CA, USA, 24–29 July 2011, pp. 1–7.
Mazo M and Tabuada P (2011) Decentralized event-triggered control over wireless sensor/actuator networks. *IEEE Transactions on Automatic Control* 56(10): 2456–2461.
Okou F, Dessaint LA and Akhrif O (2005) Power systems stability enhancement using wide-area signals based hierarchical controller. *IEEE Transactions on Power Systems* 20(3): 1465–1477.
Sahoo A, Xu H and Jagannathan S (2013) Adaptive event-triggered control of an uncertain linear discrete time system using measured input and output data. In: *American Control Conference*, Washington, DC, USA, 17–19 June 2013, pp. 5672–5677.
Sahoo A, Xu H and Jagannathan S (2016) Neural network-based event-triggered state feedback control of nonlinear continuous-time systems. *IEEE Transactions on Neural Networks and Learning Systems* 27(3): 497–509.
Tahir M and Mazumder SK (2015) Self-triggered communication enabled control of distributed generation in microgrids. *IEEE Transactions on Industrial Informatics* 11(2): 441–449.
Taylor CW, Erickson DC, Martin KE, Wilson RE and Venkatasubramanian V (2005) WACS-wide-area stability and voltage control system: R&D and online demonstration. *Proceedings of the IEEE* 93(5): 892–906.
Wang L and Cheung H (2008) Model prediction adaptive control for wide-area power system stability enhancement. In: *Power and Energy Society General Meeting – Conversion and Delivery of Electrical Energy in the 21st Century*, Pittsburgh, PA, USA, 20–24 July 2008, pp. 1–8.
Wen S, Yu XH, Zeng ZG and Wang JJ (2016) Event-triggering load frequency control for multi-area power systems with communication delays. *IEEE Transactions on Industrial Electronics* 63(2): 1308–1317.
Wu H, Wang Q and Li XH (2008) PMU-based wide-area damping control of power systems. In: *Joint International Conference on Power System Technology and IEEE Power India Conference*, New Delhi, India, 12–15 October 2008, pp. 1–4.
Xiao XQ, Wang FF and Zhao HS (2011) Application of self-triggered control in power system excitation control. In: *International Conference on Electrical and Control Engineering*, Yichang, China, 16–18 September 2011, pp. 577–580.
Zhang H, Hong QQ, Yan HC and Yang FW (2016) Event-based distributed H-infinity filtering networks of 2DOF quarter-car suspension systems. *IEEE Transactions on Industrial Informatics* 13(1): 1–9.
Zhang J, Chung CY and Han YD (2012) A novel model decomposition control and its application to PSS design for damping inter-area oscillations in power systems. *IEEE Transactions on Power Systems* 27(4): 2015–2025.

Appendix

Proof of Theorem 1: For the simplicity, the subscript of time t is omitted in this part. Besides, some derivation processes are excluded owing to the page limit. Consider the Lyapunov function candidate given as $L(\Delta y) = \Delta y^T P \Delta y$ where P satisfies the Lyapunov equation (7). Taking the first derivative, we have

$$\dot{L}(\Delta y) = \Delta \dot{y}^T P \Delta y + \Delta y^T P \Delta \dot{y} \tag{A.1}$$

According to the system state space representation derived in (4), (A.1) can be represented as

$$\dot{L}(\Delta y) = \left[A_y \Delta y + B_y \Delta u\right]^T P \Delta y + \Delta y^T P \left[A_y \Delta y + B_y \Delta u\right] \tag{A.2}$$

Recall the event-triggered control designed in (6), (A.2) can be expressed as

$$\begin{aligned}
\dot{L}(\Delta y) &= \left[A_y \Delta y + B_y K(e + \Delta y)\right]^T \\
&\quad P \Delta y + \Delta y^T P \left[A_y \Delta y + B_y (e + \Delta y)\right] \\
&\le \Delta y^T \left(A_y + B_y K\right)^T P \Delta y + \Delta y^T P \left(A_y + B_y K\right) \Delta y \\
&\quad + e^T K^T B_y^T P \Delta y + \Delta y^T P B_y K e \\
&\le \Delta y^T \left[\left(A_y + B_y K\right)^T P + P \left(A_y + B_y K\right)\right] \Delta y \\
&\quad + e^T K^T B_y^T P \Delta y + \Delta y^T P B_y K e \\
&\le \Delta y^T Q \Delta y + e^T K^T B_y^T P \Delta y + \Delta y^T P B_y K e \\
&\le -q \|\Delta y\|^2 + \left\|2 P e^T B_y K\right\| \|\Delta y\| \|e\|
\end{aligned} \tag{A.3}$$

According to the event-triggering condition derived in (9), we have

$$\begin{aligned}
\dot{L}(\Delta y) &\le -q \|\Delta y\| + \gamma_{ideal} 2 \left\|P e^T B_y K\right\| \|\Delta y\|^2 \\
&\le -q \|\Delta y\|^2 + \sigma q \|\Delta y\|^2 \le -(1 - \sigma) \|\Delta y\|^2
\end{aligned} \tag{A.4}$$

Since $0 < \sigma < 1$, the derived event-triggering condition can guarantee that the system is asymptotically stable.

Proof of Theorem 2: Selecting the Lyapunov function candidate as $L(\Delta y) = \Delta y^T P \Delta y$ where P satisfies the Lyapunov equation (7). According to the system state space representation derived in (5), taking the first derivative, we have

$$\begin{aligned}
\dot{L}(\Delta y) = &\left[\left(A_y + \Delta A\right) \Delta y + \left(B_y + \Delta B\right) \Delta u + D\right]^T P \Delta y \\
&+ \Delta y^T P \left[\left(A_y + \Delta A\right) \Delta y + \left(B_y + \Delta B\right) \Delta u + D\right]
\end{aligned} \tag{A.5}$$

Recall the event-triggered control designed in (6) in the paper, (A.5) can be expressed as

$$\begin{aligned}\dot{L}(\Delta y) &= \left[\left(A_y + \Delta A\right)\Delta y + \left(B_y + \Delta B\right)Ke + \left(B_y + \Delta B\right)K\Delta y + D\right]^T P\Delta y + \Delta y^T P\left[\left(A_y + \Delta A\right)\Delta y + \left(B_y + \Delta B\right)Ke + \left(B_y + \Delta B\right)K\Delta y + D\right] \\ &\leq \Delta y^T Q\Delta y + \Delta y^T(\Delta A + \Delta BK)^T P\Delta y + \Delta y^T P(\Delta A + \Delta BK)\Delta y + e^T K^T\left(B_y + \Delta B\right)^T P\Delta y + \Delta y^T P\left(B_y + \Delta B\right)Ke + 2D_M\|P\| \\ &\leq -q\|\Delta y\|^2 + 2\|P\|(a_u + b_u\|K\|)\|\Delta y\|^2 + \left\|2PB_yK\right\|\|\Delta y\|\|e\| + \|2P\Delta BK\|\|\Delta y\|\|e\| + 2D_M\|P\|\end{aligned} \tag{A.6}$$

According to the event-triggering condition derived in (9) in the paper, we have

$$\begin{aligned}\dot{L}(\Delta y) &\leq -q\|\Delta y\|^2 + 2\|P\|(a_u + b_u\|K\|)\|\Delta y\|^2 + \gamma_T\left(\left\|2PB_yK\right\| + \|2P\Delta BK\|\right)\|\Delta y\|^2 + 2D_M\|P\| \\ &\leq -(q - \Phi)\|\Delta y\|^2 + \gamma_T\left(\left\|2PB_yK\right\| + \|2P\Delta BK\|\right)\|\Delta y\|^2 + 2D_M\|P\| \\ &\leq -(1 - \sigma)(q - \Phi)\|\Delta y\|^2 + b_e\end{aligned} \tag{A.7}$$

Since $0 < \sigma < 1$ and $\Phi < q$, the derived event-triggering condition can guarantee that the uncertain system is UUB with bounds given in (11) in the paper.